

Development of a Human-Friendly Omni-directional Wheelchair with Safety, Comfort and Operability Using a Smart Interface

¹Kazuhiko Terashima, ²Juan Urbano, ³Hideo Kitagawa,
and ¹Takanori Miyoshi

¹*Toyohashi University of Technology*

²*Denso Preas*

³*Gifu National College of Technology*
Japan

1. Introduction of the OMW

A variety of wheelchairs with different options and special add-on features have been developed to meet a wide range of needs (Pin & Killough, 1994), (Wada & Asada, 1999), (West & Asada, 1992). In order to satisfy the demand for higher mobility, designers have created new driving concepts such as omni-directional movement which allows any combination of forward, sideways, and rotational movement, thus ensuring users much more freedom and safety in wide or narrow spaces.

Autonomous electric wheelchairs are very useful for people who cannot move their upper bodies freely. However, these wheelchairs need to be fitted with a central control unit and high-level sensors capable of realizing complex navigation and obstacle avoidance tasks, based on a description of the environment and final goals marked out by those sensors. Since autonomous wheelchairs can function well only in special environments, this mode greatly limits the user's freedom.

In order to offer users with a higher degree of independence, the user-controlled movement mode, or semi-autonomous mode, which is operated under absolute user control by an input device such as a joystick, switch, monitor, etc., has been developed. The main difference between autonomous and semi-autonomous systems is that in semi-autonomous systems users interact in real time to perform certain tasks in dynamic environments. Under user control, the wheelchair can go wherever the user wants it to. Therefore, this mode provides a high degree of user independence.

However, it is necessary to keep in mind that some elderly people or handicapped people can not use their arms due to weakness or injury. These people need the help of an attendant. In developed countries in which the number of young people is declining yearly, some healthy elderly people are taking care of other elder or handicapped people. For these attendants, a system that helps them to push the wheelchair and its occupant would be very convenient.

Years ago, the main purpose of research was to develop reliable systems without showing great concern for the comfort of the user when employing them. However, with the advent of ergonomics or "the systematic application of knowledge about the psychological, physical, and social attributes of human beings in the design and use of all things which affect a person's working conditions: equipment and machinery, the work environment and layout, the job itself, training and the organization of work", designers have become more aware of the importance of the user when designing any device. Comfort, or "a state of being relaxed and feeling no pain, when using a piece of equipment" emerged as a design goal. This is especially true in the case of wheelchairs where the occupants are weak people because of age or disease.

Therefore, the development of an omni-directional wheelchair that can provide the occupant with semi-autonomous functions and comfort; and the attend with power assist support is highly desirable.

When considering about wheelchairs, it is necessary to remember that they can be classified in two main groups: manual wheelchairs or wheelchairs that move due to the application of force by the occupant, and electric wheelchairs, or wheelchairs that employ electric energy for generating movement. Just the latter are the object of interest for this research.

In order to offer users with a higher degree of independence, the user-controlled movement mode, or semi-autonomous mode, which is operated under absolute control of users by an input device such as joystick, switch, monitor, etc., has been developed. Under control of users, wheelchair can go wherever users want to go. Therefore, this mode provides a great independence to users. For achieving reliable navigation, obstacle detection and collision avoidance must be considered when designing a wheelchair. In the case of semi-autonomous wheelchairs, most of them rely on reactive obstacle avoidance (Argyros et al., 2002), (Borgolte et al., 1998), (Levine et al., 1999), (Tahboub, 2001), (Yanco et al., 1995) which is in some degree safe but uncomfortable for the user if he is not aware of the obstacle and he is unexpectedly taken away from it. "Not being aware" means that the user is not giving attention to the environment or maybe he is a blind one. It means that environment information must be provided in a way that it can be perceived without using the eyes. Most of semi-autonomous wheelchairs use joysticks as input devices then it appears natural to provide environment information to users through joystick. That is, joystick becomes a haptic device, or a device that provides information through the sensation of touch.

Many power-assisted wheelchairs have been developed for handicapped people who have free use of their arms. Power assist is useful for reducing the burden of manual workers and elderly people. In recent years, it is necessary for elderly people to support other elderly people. Research on power-assist systems has been widely reported (Hayashibara et al., 1999), (Kawai et al., 2004), (Kumar et al., 1997), (Lee et al., 1999), (Naruse et al., 2005) and much study has been devoted to wheelchairs (Sanada et al., 2005), (Seki et al., 2005), (Wu et al., 2004) regarding the chair's straight-line forward and backward movement. However, in spite of its importance, little study has focused on power-assist with respect to rotation, lateral and slanting movements. The application of power-assist for supporting the attendant of an omni-directional wheelchair constitutes a new area of research. Though some research regarding a power-assist system for omni-directional vehicles related to carts is available (Maeda et al., 2000), no report regarding this topic as related to wheelchairs has appeared, to the authors' knowledge. In the case of the Omni-directional Cart with Power-assist System developed by Matsushita Electric Works (Maeda et al., 2000) a cart with the

length being bigger than the width is considered. In this case, they report problems with lateral motion when the length of the cart is very big. Moreover, it looks like they have considered turning, but not rotation over the center of gravity because it could not be possible due to the dimensions of the cart. On the other hand, achieving almost perfect rotation over the center of gravity and high accuracy in lateral and forward-backwards motion is a very important goal in this research.

In recent years special attention has been given to ride comfort. When ride comfort is studied, most of them consider only influences of vibration in up-down direction caused by unevenness of the ground. Various alternatives have been mooted to solve this problem, however, most of them are based on more or less complex mechanical solutions such as soft cushions, vibration absorber, etc. (Sato et al., 2003). With the use of these advanced equipments, the cost has been increased accordingly and, moreover, it also usually increases the weight of the device. According to literature, when automobile drivers were asked about parameters necessary to driving comfort, they mentioned factors such as a well designed seat, adjustable features, correct temperature, ease of reaching controls and pedals, enough space, low noise level as well as vibration-free riding.

For wheelchair users, the factors related to comfort are almost the same as those mentioned above. In fact, two main problems are considered when designing a comfortable wheelchair: comfortable seat design and suppression of vertical vibration caused by rough pavement or the wheelchair's mechanical elements. However, there is another factor that must be considered: vibration due to jerking, or the variation of linear acceleration (Seki et al., 2005). When the natural frequency of this vibration synchronizes with the natural vibration frequency of human beings, the resonance phenomenon causes large oscillations and therefore leads to the discomfort of the wheelchair's occupant. In past studies (Matsuoka, 2000a), (Matsuoka, 2000b), (Nishiyama, 1993), (Okada, 1980), (Smith, 2000), the user's upper body is considered as a series of rigid segments (head, chest, waist) connected by flexible joints. Each joint is given a rotational spring constant (RSC) and a rotational viscous damping constant (RVDC). However, since waist is connected to the seat directly, its swing frequency is much less than that of head and chest. Then, in this research, in order to simplify the model, it is considered that upper human body consists of two rigid segments: head and torso. Moreover, in this research the human model is used for studying vibration of the human body when it moves in a horizontal plane, while previous researchers have used a human model for studying the problem of vibration of the human body when it moves in a vertical direction.

In author's laboratory, a holonomic Omni-directional Wheelchair (OMW) which can act as an autonomous (Kitagawa, Terashima et al., 2002), semi-autonomous (Kitagawa, Terashima et al., 2001) or power assisted (Kitagawa, Terashima et al., 2004) wheelchair has been developed. Because of its omni-directional movement, it is able to navigate smoothly in structured inner environments using range sensors for getting environment information. In order to recognize surrounded environment it can build a local map which provides distance to nearest obstacles. In semi-autonomous mode the input device is a joystick, with velocity of OMW being proportional to the angular displacement of the joystick. In previous research, just the idea of haptic feedback was proposed (Tahboub, 2001), or a combination of a haptic joystick with a virtual simulator for navigation was used (Protho et al., 2000). In this research, a wheelchair provided with a haptic joystick has been built. Moreover impedance of joystick or force feedback changes according not only to velocity of OMW but also to the

distance of OMW to the nearest obstacle in the direction of movement. The nearest the distance becomes, the more difficult it becomes to move the joystick, then the user understands that he is going to collide against an obstacle soon and he can decide to change the direction of movement or to stop OMW. The proposed approach by haptic joystick has been tested with good results (Kitagawa, Terashima et al., 2001), and furthermore, a novel navigation guidance system to induce evasive movement, while the omni-directional wheelchair performs slide movement without rotated movement, using the haptic feedback joystick is proposed. The obstacle existing toward the moving direction of vehicle has possibility of collision. Therefore, when the obstacle exists in the direction of the OMW's movement, this approach gives the joystick force to operator's hand such that induces evasive movement to navigate OMW toward the direction without obstacle for operator's safe and smooth driving. The purpose of this study gives a support system to realize operator's safe and smooth driving when the operator passes through the narrow aisle, entrance of room, or enters an elevator, etc. (Kondo, et al. 2008).

In the power assisted mode, in the authors' laboratory (Kitagawa, Terashima et al., 2004) a six-axis force sensor is used for measuring the force applied by the attendant in two orthogonal axes, X and Y, and a rotational direction θ . This force is then changed to reference velocity V_x , V_y , and ω by using a first-order lag controller. Finally, the reference velocity is applied to the servo-motors of the OMW. This system works well as a power-assist system, and provides the attendant effective support. However, a problem related to the operability of the OMW remains. Due to the application of the power-assist system, the operability of the OMW diminishes especially when the attendant tries to rotate the chair in a clockwise (CW), or counter-clockwise (CCW) direction around the OMW's center of gravity CG.

A survey was conducted among various attendants trying to discover some relationships in the way they developed forwards-backwards, lateral, and rotational movements. It was impossible to find general rules that explained all cases, but a relationship was found between lateral and rotational movements. These relationships were used as the basis for constructing a fuzzy reasoning system (Mathworks, 2002), (Harris et al., 1993), (Mamdani & Assilian, 1985), (Shaw, 1998), (Sugeno & Kang, 1998), (Takagi & Sugeno, 1985) that helped to improve the operability of the OMW. An expert operator can move the OMW with ease, but for people not accustomed to its use it is difficult to easily manage in any direction. Thus, the development of a novel power-assist system with easy operability is strongly demanded. In this paper, this system is called a "skill-assist system" (Yamada et al., 2002).

Nevertheless, when the system was tested by different attendants, a completely satisfactory result was not obtained by every attendant, since each operator has his or her own tendencies, and thus the parameters of the fuzzy inference system must be reasonably tuned to respond to the individual. Tuning the fuzzy inference system by trial and error was thus attempted and its results reported in (Kitagawa, Terashima et al., 2004). This was found to be a time-consuming process, leading to fatigue and boredom in the attendants.

Hence, a better tuning method, a method that allows tuning of the fuzzy inference system, is needed. This can be obtained by adding Neural Networks (NN) to the fuzzy inference system, obtaining what is known as a neuro-fuzzy system. Much research has been devoted to this topic (Jang, 1993), (Jang et al., 1997), (Juang & Lin, 1998), (Lian et al., 1999), (Lin & Lee, 1991), (Nguyen et al., 2003). Jang (Jang, 1993) developed the ANFIS (Adaptive-Neuro-Network-based Fuzzy Inference System), a neuro-fuzzy system in which the fuzzy inference

system is tuned by using the system's input data. Tuning is performed by minimizing the output error of the NN used in combination with the fuzzy inference system. For achieving this goal, the NN is trained by using a hybrid method that combines least squares and the Backpropagation algorithm (BP law). This method is thus thought to be an effective method for tuning the parameters of the OMW's fuzzy inference system.

In the case of comfortable navigation, in the authors' laboratory comfort has been a subject of study in the autonomous mode without the joystick (Terashima et al., 2004) but only when the OMW moves in a single direction, X or Y. In the present paper, comfort is studied when the OMW moves in any direction, such as a slanting direction, when in practical semi-autonomous operation mode using the joystick (Urbano et al., 2005b). For the command input via joystick operation, the velocity control of the OMW is carried out by means of frequency shaping using the Hybrid Shape Approach (HSA) proposed by the authors (Yano et al., 2000) in order to achieve the swing suppression control or comfortable driving by excluding a specific spectrum of elements such as the natural frequency of the OMW and the discomfort frequency of human organs. A human model which considers the human upper body to be composed of two parts, the torso and head, has been developed and used in order to test the effectiveness of the proposed approach.

In this chapter, in section 2, kinematics and dynamics of the OMW are described. In section 3, semi-autonomous operation and guidance system of the OMW for obstacle avoidance by haptic joystick. In section 4, power assist control of OMW for helper and, in section 5, adaptive control by Neuro-Fuzzy system of OMW using a touch Panel as human interface for realizing tailor-made vehicle. In section 6, comfort driving of the OMW and conclusion in section 7.

2. Kinematics and dynamics of the OMW

The OMW, which can act as an autonomous (Kitagawa et al., 2002), semi-autonomous (Kitagawa et al., 2001) or power assisted (Kitagawa et al., 2004) wheelchair is shown in Fig. 1, and its specifications are shown in Table 1.



Fig. 1. Omni-directional wheelchair (OMW)

The OMW is able to move in any arbitrary direction without changing the direction of its omni-wheels, which are shown in Fig. 2. In this system, four omni-directional wheels are

individually driven by four motors, as shown in Fig. 3. Each wheel has passively driven free rollers at its circumference. The wheel that rolls perpendicularly to the direction of movement does not stop its movement, because of the passively driven free rollers. These wheels thus allow movement that is holonomic and omni-directional.

Size	Width	0.70 [m]
	Depth	1.50 [m]
	Height	1.10 [m]
Weight		70 [kg]
Maximum velocity		1.0 [m/s]
Maximum acceleration		0.5 [m/s ²]

Table 1. Specifications of the OMW



Fig. 2. Omni-wheel

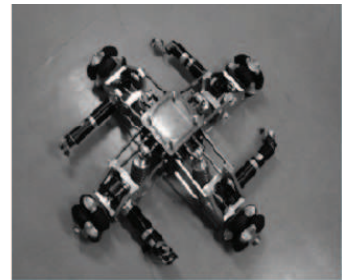


Fig. 3. Omni-wheels and motors

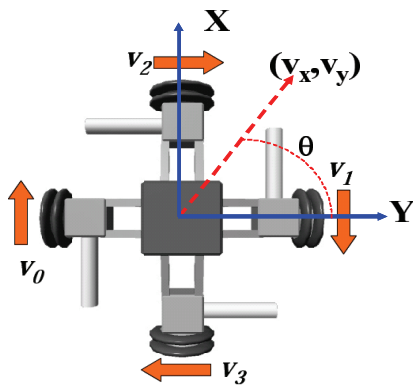


Fig. 4. Velocity vectors of the omni-wheels

In the coordinate system of the OMW, the X-axis is defined when the OMW moves forward or backward. The Y-axis is defined when the OMW moves to the right or left, and rotational

direction is defined according to direction θ perpendicular to the plane determined by X and Y. The joystick's coordinate system is established in the same way as that of the OMW. Furthermore, if V_x is the velocity of the OMW in the X-axis, V_y the velocity of the OMW in the Y-axis, and ω the angular velocity of the OMW when it rotates around the vertical axis, the velocity of the OMW can be expressed as $V_{OMW} = [V_x, V_y, \omega]^T$. The velocity of the OMW is the vectorial sum of the velocities of the four omni-directional wheels. The velocity vector for the omni-wheels is written as $V_{WHEEL} = [V_0, V_1, V_2, V_3]^T$. The velocity vectors corresponding to each omni-wheel are shown in Fig. 1. In Fig. 4, θ is the angle that the velocity vector of the OMW has with the axis Y of the reference system.

From Fig. 4:

$$V_x = \frac{1}{2}(V_0 - V_1) \tag{1}$$

$$V_y = \frac{1}{2}(V_2 - V_3) \tag{2}$$

$$\omega = \frac{1}{4l_{ob}}(-V_0 - V_1 - V_2 - V_3) \tag{3}$$

, where l_{ob} is the distance from the center of the OMW to the circumference of the omni-wheels. Written in a matrix form, the above equations become:

$$V_{OMW} = B \cdot V_{WHEEL} \tag{4}$$

where

$$B \equiv \begin{bmatrix} \frac{1}{2} & -\frac{1}{2} & 0 & 0 \\ 0 & 0 & \frac{1}{2} & -\frac{1}{2} \\ -\frac{1}{4l_{ob}} & -\frac{1}{4l_{ob}} & -\frac{1}{4l_{ob}} & -\frac{1}{4l_{ob}} \end{bmatrix} \tag{5}$$

Since generally a matrix should be square in order to calculate its inverse, the coefficients' matrix in Eq. (4) should be square in order to calculate V_{WHEEL} from V_{OMW} . Keeping this in mind, the angular velocity ω of OMW is divided into two parts: ω_1 produced by V_0 and V_1 , and ω_2 produced by V_2 and V_3 .

$$\omega_1 = \frac{1}{2l_{ob}}(-V_0 - V_1) \tag{6}$$

$$\omega_2 = \frac{1}{2l_{ob}}(-V_2 - V_3) \quad (7)$$

$$\omega = \frac{1}{2}(\omega_1 + \omega_2) \quad (8)$$

By using Eq. (6), Eq. (7) and Eq. (8), it is possible to get:

$$\begin{bmatrix} V_x \\ V_y \\ \omega_1 \\ \omega_2 \end{bmatrix} = \begin{bmatrix} \frac{1}{2} & -\frac{1}{2} & 0 & 0 \\ 0 & 0 & \frac{1}{2} & -\frac{1}{2} \\ -\frac{1}{2l_{ob}} & -\frac{1}{2l_{ob}} & 0 & 0 \\ 0 & 0 & -\frac{1}{2l_{ob}} & -\frac{1}{2l_{ob}} \end{bmatrix} \begin{bmatrix} V_0 \\ V_1 \\ V_2 \\ V_3 \end{bmatrix} \quad (9)$$

V_{OMW} can be expressed by:

$$\begin{bmatrix} V_x \\ V_y \\ \omega \end{bmatrix} = \begin{bmatrix} 1 & 0 & 0 & 0 \\ 0 & 1 & 0 & 0 \\ 0 & 0 & \frac{1}{2} & \frac{1}{2} \end{bmatrix} \begin{bmatrix} V_x \\ V_y \\ \omega_1 \\ \omega_2 \end{bmatrix} \quad (10)$$

For avoiding the slippage of the wheels, the constraint $\omega_1 = \omega_2$, or $V_0 + V_1 = V_2 + V_3$ is imposed. By considering $\omega_1 = \omega_2$, Eq. (9) can be expressed as follows:

$$V_{WHEEL} = B^{*-1} \cdot V_{OMW} \quad (11)$$

, where

$$B^{*-1} \equiv \begin{bmatrix} 1 & 0 & -l_{ob} \\ -1 & 0 & -l_{ob} \\ 0 & 1 & -l_{ob} \\ 0 & -1 & -l_{ob} \end{bmatrix} \quad (12)$$

Here, B^{*-1} is a pseudo-inverse matrix that allows the velocity of each wheel to be obtained based on the velocity of the OMW.

3. Semi-autonomous Operation and Guidance System of the OMW for Obstacle Avoidance by Haptic Joystick.

The OMW is able to move in any arbitrary direction without changing the direction of the wheels. In this system, four omni-directional wheels are individually driven by four motors.

Each wheel has passively driven free rollers at its circumference. The wheel that rolls perpendicularly to the direction of movement does not stop its movement because of the passively driven free rollers. Thus, these wheels allow holonomic and omni-directional movement.

The obstacle detection sensors are activated in back and forth of the OMW in order to obtain information regarding its surrounding environment. In this research, the input device is a joystick. The direction of the vehicle movement depends on orientation of the joystick and speed is proportional to declination of the joystick. Moreover, two motors are installed in each x and y axis of the joystick, and the joystick can give virtual spring damper characteristics because of the impedance control. (Kitagawa et al, 2001), (Urbano et al, 2005a).

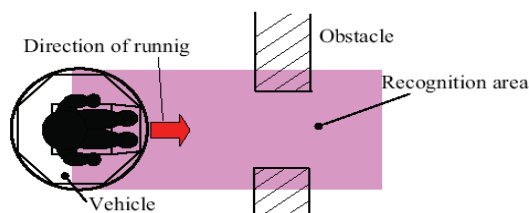


Fig. 5. Schematic diagram of environmental recognition and navigation

It is possible to acquire the surrounding environmental information in real time by two obstacle detection sensors. The obstacle with danger collision exists in the direction of OMW's running with current input. Therefore, the algorithm that chooses only environmental information which exists in the direction of the OMW's running from all of the obtained information is constructed. Figure 5 shows the outline of the environmental recognition system. The recognition area can be changed, corresponding to the direction of OMW's running.

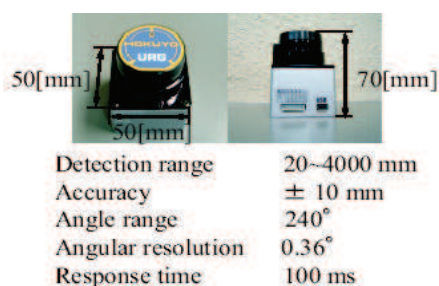


Fig. 6. Specification of obstacle detection sensor

The specifications of the obstacle detection sensor "URG-04LX" (Hokuyo Automatic Co. Ltd.) are shown in Fig. 6. This sensor gives real-time updates of the surrounding environment. The sensor covers a wide angular range. The maximum angular resolution on

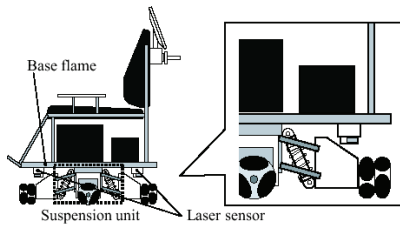


Fig. 7. Configuration of obstacle detection sensor (1)

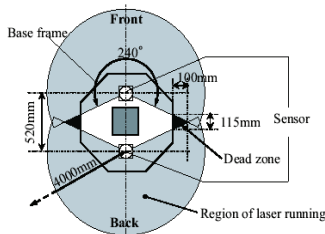


Fig. 8. Configuration of obstacle detection sensor (2)

the sensor is 0.36 [deg] within range of 240 [deg]. And measurement range of the sensor is 20-4000 [mm]. Furthermore, it only takes 100 [ms] for one complete scan. In this research, the angular resolution is applied 3.6 [deg] for the brevity of calculations. Two sensors are attached on frontside and backside of the base frame, where the control unit, the chair and the battery is installed, as shown in Fig. 7. It is possible to get the surrounding environmental information without shielding matters, because the unit above the base frame is braced with the suspension unit at the OMW's center, as shown in Fig. 4. Then, there are small dead areas in laser sensors' scanning in OMW's right and left sides, as shown in triangle black zone in Fig. 8. These dead areas are regarded as a part of OMW as described later. The total output response time to capture environmental map is 200 [ms] in this system, because of using two obstacle detection sensors. Take into account of the velocity of OMW's movement and velocity response of OMW, the response time is of no matter.

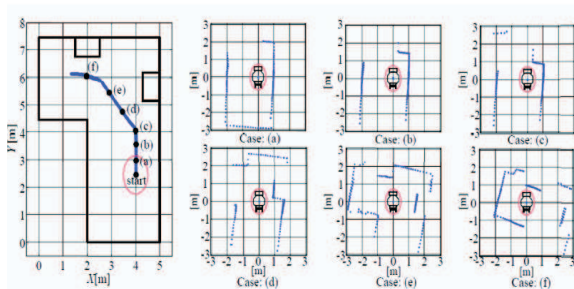


Fig. 9. Experimental result of obtaining environmental information

Figure 9 shows experimental results of obtaining environmental information using the obstacle detection sensor, while human operates the joystick for navigation. In this experiments, the OMW is manually controlled using joystick by operator. Note that, the obstacle and wall is recognized as points, and the map described by points is rotated while OMW is skew movement. It should be considered that this phenomenon is caused by slipping of the omni-wheel and differences in the diameter of each four omni-wheels. In this section, the algorithm that choses only environmental information existing toward the moving direction of the OMW from all the surrounding environmental information is presented.

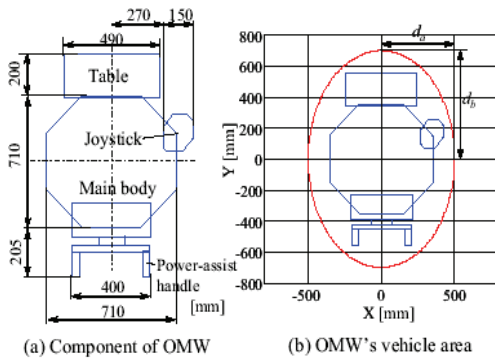


Fig. 10. Definition of OMW's vehicle area

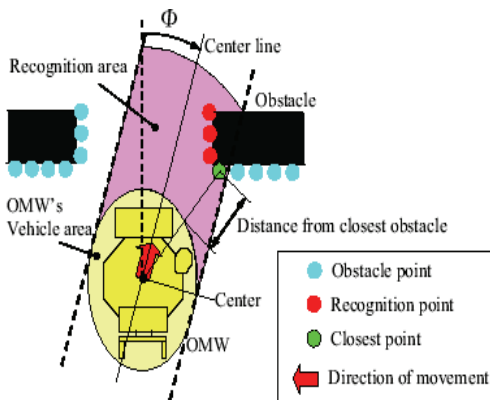


Fig. 11 . The environmental recognition system

First, the OMW's vehicle area which covers the entire OMW is defined. Since the OMW has a table, the joystick, and the power-assist handle, the OMW's vehicle area is defined as the shape of an ellipse covering both parts of OMW's main body and the dead areas of laser scanning as shown in Fig. 7(a). The length of shorter axis of this ellipse is $d_a = 0.5$ [m] and

longer axis is $d_b = 0.7$ [m], as shown in Fig. 7. If the obstacle goes inside the OMW's vehicle area, it is considered as a crashing obstacle. Next, an algorithm such that only environmental information existing toward the moving direction of the OMW is chosen, is proposed. Now the OMW is slide moving in direction Φ , as shown in Fig. 11. Then the surrounding environmental information is acquired as a set of points by two obstacle detection sensor. These points set are defined as the obstacle points. The straight line drawn by extending the moving direction from the OMW's center point is defined as the center line. The area between two lines such as being parallel to the center line and tangent to the oval vehicle area, is defined as the recognition area. And the obstacle points existing in the recognition area are defined as the recognition points. The closest recognition point to the OMW's vehicle area is defined as the closest point. Thus, the obstacle existing in the recognition area has danger of collision with OMW. By means of this algorithm, the present system can recognize only the obstacle with possibility of collision of the present moving direction, and teach the distance to the closest recognition point to the OMW. And the environmental recognition system achieves high speed response time to capture environmental map, compared with velocity response of OMW. Therefore, if navigator suddenly changes the joystick's direction, navigator's safe is assured with the presented system.

Derivation of the recognition area is explained in more detail. Now, the vehicle is moving in the direction Φ . A perfect circle shape is defined as the vehicle area. In this algorithm, the vehicle area needs to be perfect circle, but the OMW's vehicle area is really ellipse shape. Therefore, in order to change the shape of OMW's vehicle area into a perfect circle shape, the scale of X-axis or Y-axis is temporarily altered while picking the recognition point. For example, in this study case, all of Y-coordinate value of obstacle points times d_a/d_b , because the OMW's vehicle area is defined as shape of an ellipse, and the length of shorter axis is $d_a = 500$ [mm] on the X-axis and longer axis is $d_b = 700$ [mm] on the Y-axis, as shown in Figure 7. And movement direction Φ is converted into Φ' by following equation (dash " ' " indicates the transformed scale of X-Y axis).

$$\Phi' = \tan^{-1} \left(\frac{\sin \Phi}{d_a / d_b \cdot \cos \Phi} \right) \quad (13)$$

First, the circumference of the vehicle is divided into the layer of l thick ($L1;L2;...;Ln$) and the obstacle points are stored in these layer. Next, the range of angular is derived in several layers such as

$$\Phi' - \theta'_n \leq \Theta'_n \leq \Phi' + \theta'_n, \quad (n = 1,2,3...n) \quad (14)$$

$$\theta'_n = \sin^{-1} \left(\frac{r + nl}{r} \right) \quad (15)$$

The range of angular Θ'_n is indicated the range of the recognition area on n^{th} layer. If the obstacle point exists in the recognition area, this point is defined as the recognition point.

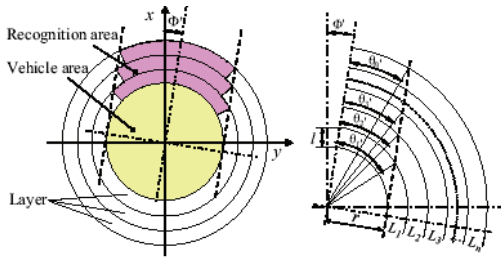


Fig. 12. Definition of recognition area

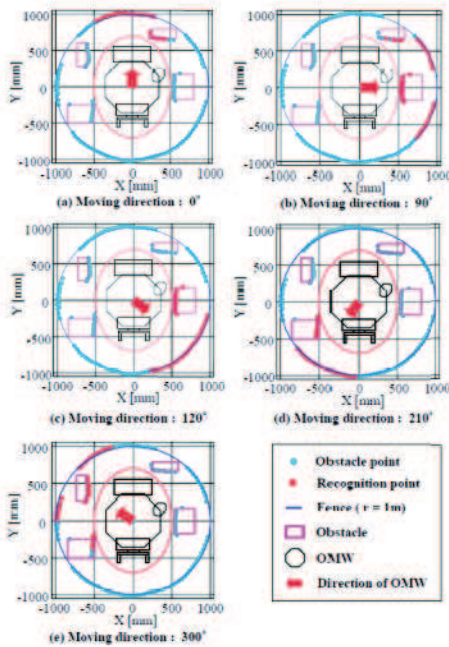


Fig. 13. Experimental results of environment recognition system

After picking the recognition points from all of the obstacle point with the use of above algorithm, all of the Y-coordinate value of obstacle points and recognition points times d_b/d_a in order to reconvert the transformed scale of X-Y axis. The experiment of the environmental recognition system with the recognition area is conducted. The OMW is installed at the center of the fence of radius 1 [m], and four obstacles are installed between the OMW and the fence. The fence is made of white board. The result of this experiment is shown in figure 10. Then, the thickness of the layers is $l = 50$ [mm]. Note that, the width of the recognition area is changed to fit the OMW's vehicle area defined as shape of an ellipse, and this system can pick out the recognition points from the obstacle points.

Two motors are installed in each x and y axis of the joystick as shown in Fig. 14, and the joystick can give virtual spring-damper characteristics with the impedance control. Based on the distance to the closest obstacle and the wheelchair's input velocity, the impedance of the joystick is provided. By neglecting the effect of joint mechanical compliance and link flexibility, the desired elastic behavior can be described as

$$\tau = d\dot{q} - kq \quad (16)$$

where τ is the joystick's motor torque, d is viscous damping coefficient, k is the stiffness and q is the tilting angle from the neutral position. The viscous damping coefficient is $d = 0.015$. The desired stiffness k in the input direction of the joystick is described as the following equation, as explained in (Kitagawa et al, 2001).

$$k = k_0 \left\{ \frac{v/v_{max} + \alpha}{(r/r_{max})^2} + 1 \right\} \quad (17)$$

where v is the input velocity of the wheelchair, and r is the distance to the nearest obstacle in the input direction. The maximum input velocity is $v_{max} = 1.0$ [m/s], and the maximum distance in effectiveness range for this impedance control is $r_{max}=3.0$ [m]. The standard stiffness is $k_0 = 0.5$ [Nm/rad], and the constant value is $\alpha = 0.014$, determined considering the operator's characteristics of handling etc., as explained in (Kitagawa et al, 2001). The input direction is measured by potentiometers attached to the joystick, as shown in Fig. 15, and the distance to the nearest obstacle r is given by the environmental recognition system described above (Fig. 12).



Fig. 14. Joystick

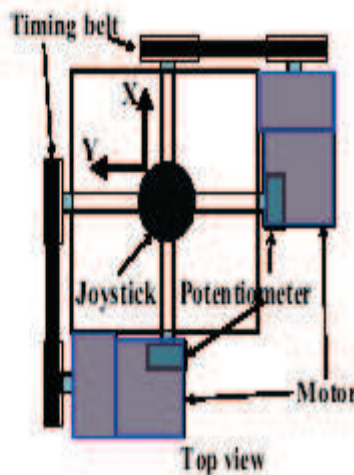


Fig. 15. Joystick system

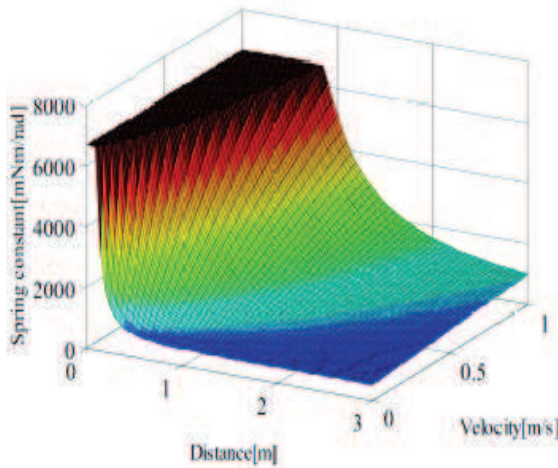


Fig. 16. Plots of stiffness against distance and velocity

Figure 16 shows plots of stiffness k against the distance r and the velocity v in the corresponding direction. Note that, as the distance r becomes smaller, the stiffness k becomes larger, moreover, as the velocity v becomes larger, the stiffness k becomes larger. In the case that the velocity is high, the motion is highly restricted, for safety. In the case that the velocity is low, the motion is scarcely restricted for maneuverability. The operator's input torque is restricted by the impedance of the joystick, hence the motion of the wheelchair is also restricted by means of the operator's joystick commands. Then, given the joystick's motor torque τ by this impedance control system is generated in the opposite direction from the declined direction of joystick by the operator.

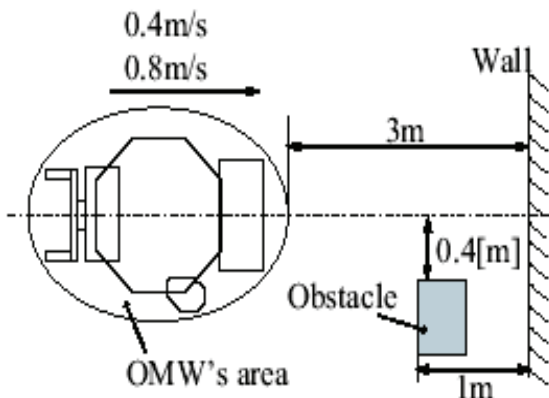


Fig. 17. Experimental condition of impedance control by using joystick

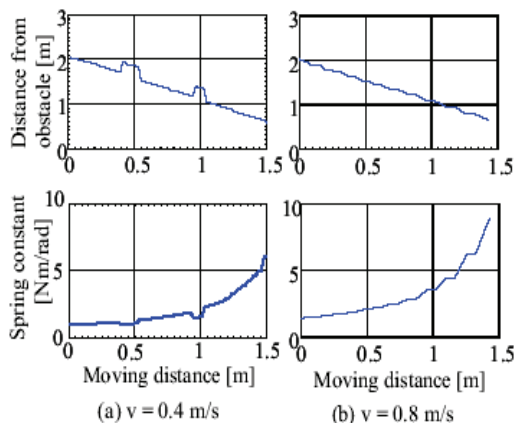


Fig. 18. Experimental result of impedance control by using joystick

Figure 18 shows an experimental result through environmental feedback using obstacle detection sensors while human operates the joystick for navigation. The stiffness k is inspected while the OMW advances toward the wall 3 [m] away from the OMW at a controlled velocity, as shown in Fig. 17. Then, the obstacle is installed between the OMW and wall. Note that, the stiffness k increases as the distance to the obstacle becomes smaller, hence the motor torque grows. Next, the stiffness k is calculated corresponding the direction of joystick's declination, using experimental result shown in Fig. 9, above.

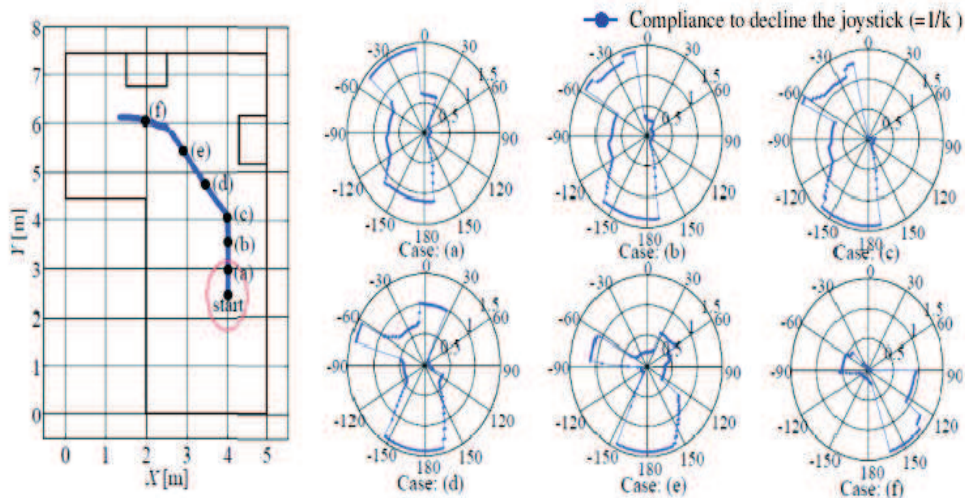


Fig. 19. Experimental result with the change of joystick's compliance during running of OMW.

Figure 19 shows the facilitation ($= 1/k$) to operate joystick for the corresponding orientation of the joystick. Then, OMW runs the speed of 0.4 [m/s]. In the sense of global coordinate as shown in the right side of Fig. 19 (case(a)-(f)), forward direction is 0 [deg], backward direction is 180 [deg], right direction is 90 [deg], and left direction is -90 [deg]. Note that, in the case that the OMW is moving in the direction nearing the obstacle, it is difficult to decline the joystick, because the motor torque grows. In other cases, it is easy to decline the joystick. Therefore the operator can naturally find out about existing obstacle and danger of collision by the present haptic device.

In the previous paragraphs, the haptic feedback joystick informs the danger level of collision to the operator. Additionally, in this section, the navigation guidance system that enable the operator to navigate the moving of OMW in the direction without crashing into obstacle, is built. This system is called the navigation guidance haptic feedback system. To begin with, take a look at the closest layer existing the recognition point.

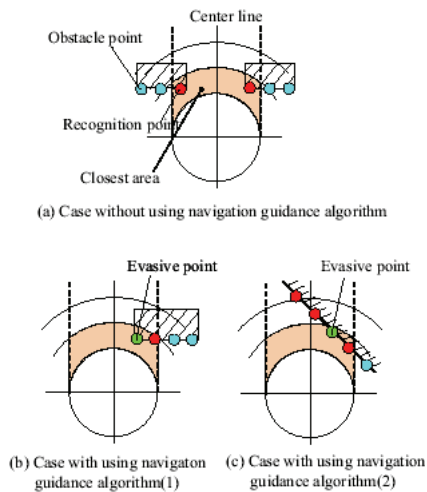


Fig. 20. Classification of cases with and without using navigation assistance algorithm

The recognition area in this closest layer is defined as the closest area, as shown in Fig. 20. Then, if the recognition points exist across the center line in the closest area, as shown in Figure 20 (a), the navigation guidance haptic feedback system is not conducted. On the other hand, if the recognition points exist on one side, as shown in Figure 20 (b) and (c), the navigation guidance haptic feedback system is worked. Moreover, in these cases (for example Figure 20 (b),(c)), the recognition points are described by polar coordinate system, and the recognition point possessing the minimum polar angle is defined as the evasive point. The OMW is controlled to move in the direction Φ by the operator's input force with the joystick, as shown in Fig. 21 (a). Using the recognition area defined previously, the inductive angle Ω_{it} with joystick is required, as shown in Fig. 21. Then the scale of Y-axis is altered, therefore, dash attached with variable indicates the changing of X-Y axis scale. For example, the evasive point is acquired in the N^{th} layer L_N (layer number is $n = N$), as shown in Figure 21 (b). In this case, the evasive point E' exists in the right side of the recognition

Thank You for previewing this eBook

You can read the full version of this eBook in different formats:

- HTML (Free /Available to everyone)
- PDF / TXT (Available to V.I.P. members. Free Standard members can access up to 5 PDF/TXT eBooks per month each month)
- Epub & Mobipocket (Exclusive to V.I.P. members)

To download this full book, simply select the format you desire below

